JACS
JOURNAL OF THE AMERICAN CHEMICAL SOCIETY

ARTICLE

pubs.acs.org/JACS

Rational Design of β-Sheet Ligands Against Aβ_{42}-Induced Toxicity

Katrin Hochdörffer,[†] Julia März-Berberich,[†] Luitgard Nagel-Steger,[‡] Matthias Epple,[†] Wolfgang Meyer-Zaika,[†] Anselm H.C. Horn,[§] Heinrich Sticht,[§] Sharmistha Sinha,[∥] Gal Bitan,[∥,⊥,#] and Thomas Schrader[†,*]

[†]Universität Duisburg-Essen, Fachbereich Chemie, Universitätstrasse 5, 45117 Essen, Germany

[‡]Universität Düsseldorf, Fachbereich Biologie, Universitätsstrasse 1, 40225 Düsseldorf, Germany

[§]Universität Erlangen-Nürnberg, Institut für Biochemie, Fahrstrasse 17, 91054 Erlangen, Germany

[∥]Department of Neurology, David Geffen School of Medicine, [⊥]Brain Research Institute, and [#]Molecular Biology Institute, University of California at Los Angeles, 635 Charles East Young Drive South, Los Angeles, California 90095, United States

Supporting Information

ABSTRACT: A β-sheet-binding scaffold was equipped with long-range chemical groups for tertiary contacts toward specific regions of the Alzheimer's Aβ fibril. The new constructs contain a trimeric aminopyrazole carboxylic acid, elongated with a C-terminal binding site, whose influence on the aggregation behavior of the Aβ_{42} peptide was studied. MD simulations after trimer docking to the anchor point (F19/F20) suggest distinct groups of complex structures each of which featured additional specific interactions with characteristic Aβ regions. Members of each group also displayed a characteristic pattern in their antiaggregational behavior toward Aβ. Specifically, remote lipophilic moieties such as a dodecyl, cyclohexyl, or LPFFD fragment can form dispersive interactions with the nonpolar cluster of amino acids between I31 and V36. They were shown to strongly reduce Thioflavine T (ThT) fluorescence and protect cells from Aβ lesions (MTT viability assays). Surprisingly, very thick fibrils and a high β-sheet content were detected in transmission electron microscopy (TEM) and CD spectroscopic experiments. On the other hand, distant single or multiple lysines which interact with the ladder of stacked E22 residues found in Aβ fibrils completely dissolve existing β-sheets (ThT, CD) and lead to unstructured, nontoxic material (TEM, MTT). Finally, the triethyleneglycol spacer between heterocyclic β-sheet ligand and appendix was found to play an active role in destabilizing the turn of the U-shaped protofilament. Fluorescence correlation spectroscopy (FCS) and sedimentation velocity analysis (SVA) provided experimental evidence for some smaller benign aggregates of very thin, delicate structure (TEM, MTT). A detailed investigation by dynamic light scattering (DLS) and other methods proved that none of the new ligands acts as a colloid. The evolving picture for the disaggregation mechanism by these new hybrid ligands implies transformation of well-ordered fibrils into less structured aggregates with a high molecular weight. In the few cases where fibrillar components remain, these display a significantly altered morphology and have lost their acute cellular toxicity.

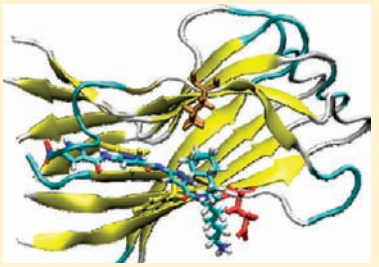

INTRODUCTION

Alzheimer's disease (AD) is a steadily increasing threat especially for industrialized countries with a growing percentage of old individuals; today an estimated 5.3 million U.S. citizens are suffering from AD, and the number is predicted to double within the next 50 years. Research on potential therapies has been going on for several decades now, without producing one single drug which is able to cure the disease. Since AD is accompanied by many diverse pathologic mechanisms, numerous avenues have been exploited in the search for a therapy. Antiinflammatory, antihypertensive, as well as hypolipidemic agents, passive and active immunization, cholinergic therapies, neuroprotective agents, glutamate receptor antagonists, β- and γ-secretase inhibitors, amyloid β-protein and tau aggregation inhibitors, metal chelating agents, monoamine oxidase inhibitors, and medicinal plants are only a subset of the most prominent classes.[1] In recent years passive immunization with Aβ-specific antibodies has held the most promise for a breakthrough; however, after a halt in phase III due to several cases of severe encephalopathy, currently running trials have yielded beneficial results only in ApoE4 carriers and still have adverse effects in quite a large number of patients. As a consequence, the call for small molecules was reinitiated.

A plethora of small molecules has been screened in the past 3 decades for their antiaggregation potential against Aβ.[2] Among these are colored heterocyclic compounds (Congo Red, cucurmin),[3] Zn and Cu chelators,[4] or peptides, in some cases taken directly from putative nucleation sites within the Aβ molecule;[5] these were often modified derivatives of the LVFFA sequence, expected to bind in a self-complementary fashion to the central hydrophobic cluster (CHC) of Aβ. Soto presented the β-sheet breaker LPFFD (iAbeta5),[6] which retained the high

Received: August 25, 2010
Published: March 07, 2011

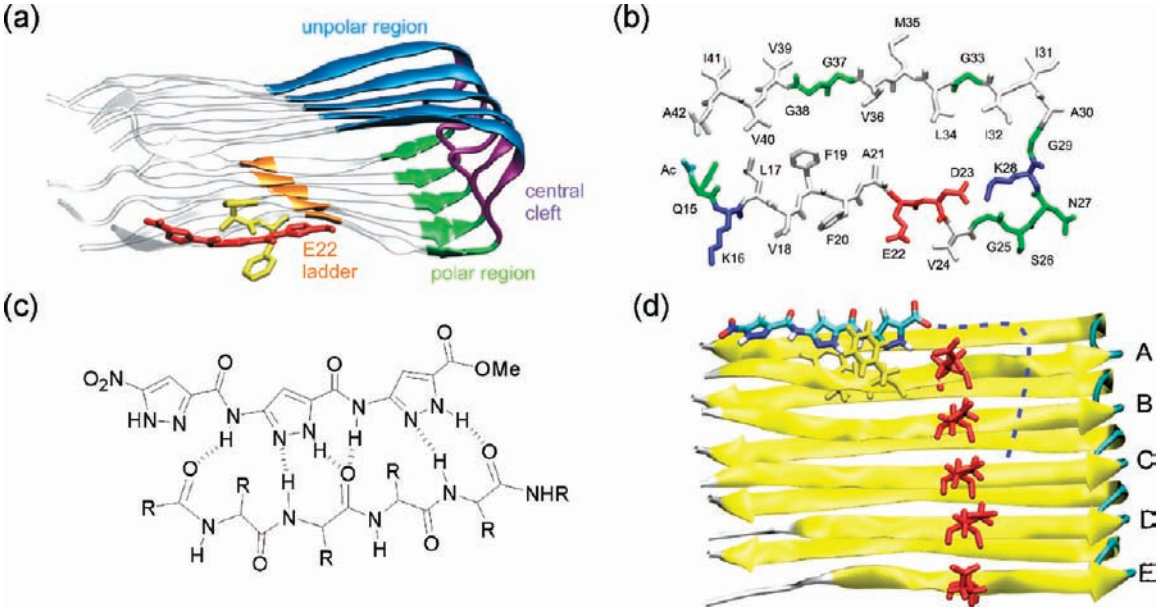

Figure 1. Structural properties of the Aβ_{42} fibril. (a) Pentameric stack from the experimentally determined Aβ_{42} fibril[15] indicating four candidate regions for the interaction of C-terminally extended aminopyrazoles. These regions are color coded in orange, green, magenta, and blue. The aminopyrazole moiety and the interacting phenylalanines are shown as red and yellow sticks, respectively. (b) Top view on one layer of the U-shaped fibril showing the location of the individual amino acids (color coding according to their biophysical properties). (c) Detailed view of the hydrogen-bonding interactions of the aminopyrazole with residues L17−A21. (d) Trimer moiety (in sticks and cpk coloring) docked to Aβ_{42}. F19/20 of chain A are depicted in yellow sticks and E22 residues of all chains (A−E) in red sticks. The dashed line indicates the orientation of ligand substituents after docking.

affinity toward the self-complementary LVFFA region (Aβ(17−21)) but impaired its β-sheet forming propensity by introducing a proline kink.

Another prominent class are peptides containing alternating N-methylated and nonmethylated peptide amides or esters, presented by Meredith, Hughes, and Kapurniotu.[7] These molecules are able to cap growing β-sheets, because their back is blocked for hydrogen bonding due to the sterically demanding *N*-methyl groups or ester oxygens. They have recently been optimized with respect to their antiaggregatory capacity by introduction of three cyclohexylglycine units and reached nanomolar IC_{50} values. The most potent compound, however, is thought to accelerate Aβ self-assembly and thereby deplete the level of neurotoxic Aβ oligomers.[8] Other more recent examples comprise the small molecule homotaurin (3-amino-1-propanesulfonic acid),[9] *scyllo*-inositol,[10] and (−)-epigallocatechin-3-gallate (EGCG).[11] Surprisingly, little knowledge/information, however, is available on the exact mechanism of action for most Aβ complexing agents, even less on experimentally verified structural details.[12] To the best of our knowledge, the only case is Sato's concept of β-sheet packing: peptide inhibitors based on a GxFxGxF framework disrupt sheet-to-sheet packing and inhibit the formation of mature Aβ fibrils.[13] This strategy was developed from inspection of solid-state NMR structures of amyloid fibrils and confirmed by ^{13}C NMR spectroscopy for the best peptide candidate in its direct complex with the 30−35 region of Aβ_{40}.

The study above emphasizes the usefulness of structural information on the Aβ topology for inhibitor design. In this context, the structures of Aβ_{40}[14] and Aβ_{42}[15] in the fibril state, which were determined by NMR spectroscopy, provide valuable insight into Aβ aggregation. With respect to the monomeric subunits, both structures consistently reveal two β-strands connected by a turn, thus forming a U-shaped topology (Figure 1a). The monomeric subunits form a longitudinal stack, thereby creating two parallel in-register β-sheets. Amyloid growing can proceed longitudinally, i.e., adsorption of new monomers along the fibril axis, and laterally, i.e., association of another stack of monomers at the lateral surface of the growing aggregate.[16]

Aminopyrazoles are rationally designed β-sheet ligands with a specific DAD sequence of hydrogen-bond donors and acceptors, perfectly complementary to that of a β-sheet.[17] In numerous experiments, they have been shown to bind selectively to the backbone of misfolded peptides in which the predominant structural element is a cross-β-sheet conformation. Several successive generations were synthesized with more than one heterocyclic binding unit for enhanced β-sheet affinity and additional charged amino acids for enhanced water solubility. A combination of two consecutive proteinogenic amino acids flanked by external aminopyrazolecarboxylates was shown to be exactly complementary to an extended β-sheet. Such derivatives were synthesized and also evaluated on the solid phase.[18] Direct interaction of dimeric and trimeric aminopyrazole derivatives with Aβ_{42} was shown and characterized by FCS, AUC, density gradient centrifugation, as well as HRMS. β-Sheet recognition as well as the individual strength of all hydrogen bonds involved were studied in great detail by R2PI spectroscopy on a cooled argon jet stream.[19] Recently, it was discovered that the trimeric aminopyrazole carboxylate could also disassemble preformed Aβ fibrils in a dose- and time-dependent manner.[20]

Concept. On the basis of the information about the Aβ-fibril topology and the mode of aminopyrazole action we decided to design a number of Trimer derivatives, which contain a variety of C-terminal extensions of the original aminopyrazole trimer. Our work includes a verification of the aminopyrazole binding site itself and application of molecular dynamics simulations to identify the binding regions of the C-terminal extensions.

dx.doi.org/10.1021/ja107675n |*J. Am. Chem. Soc.* 2011, 133, 4348–4358

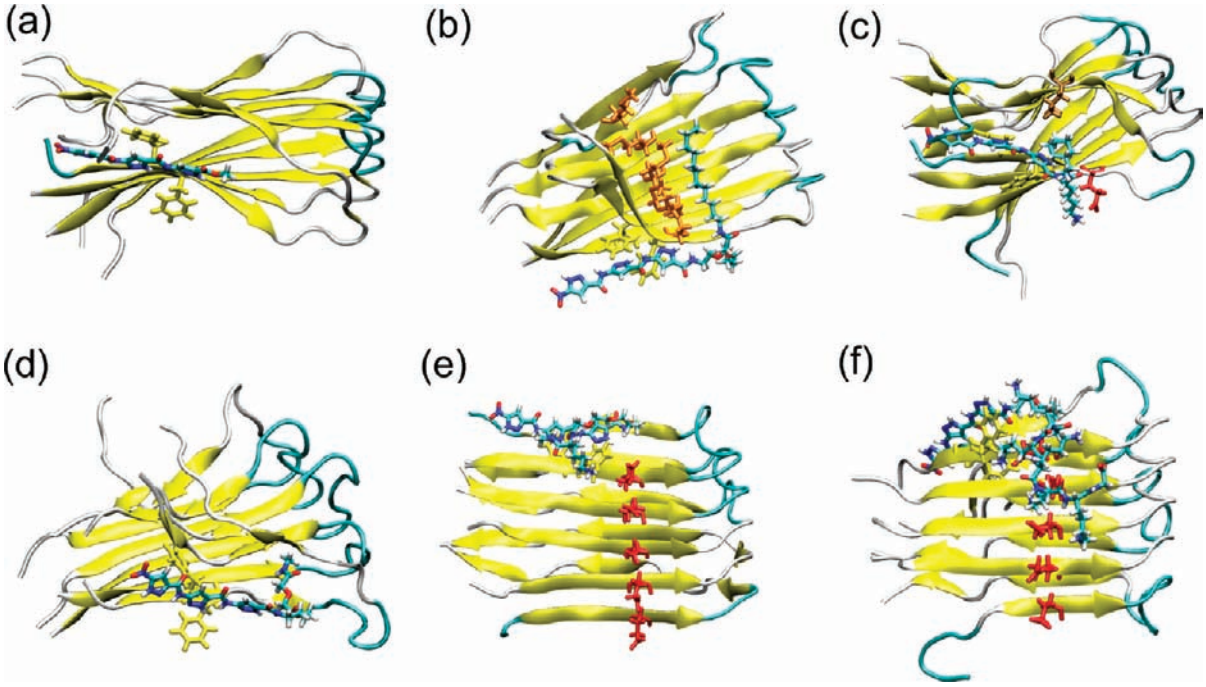

Figure 2. Final complex structures resulting from 20 ns molecular dynamics simulations of different C-terminally extended aminopyrazole ligands (cpk coloring) in complex with a pentameric Aβ_{42}-protofilament. Interacting residues are shown in stick representation: Phe19/20 (yellow), Glu22 (red), and Met35 (orange). (a) Trimer-OMe, (b) Trimer-TEG-Dd, (c) Trimer-K-Che, (d) Trimer-TEG-NHMe, (e) Trimer-TEG-K, and (f) Trimer-TEG-KKKKKG-OH.

On the basis of their binding site and the effect on the Aβ_{42} structure, the ligands can be divided in at least three distinct classes. A large variety of ligands was subsequently synthesized, and their effect on Aβ_{42} aggregation was systematically investigated with a broad range of biophysical methods. These studies revealed a close correlation between the modeled mode of binding and the experimental properties observed. To probe the relevance of these results in the environment of living cells, we tested the toxicity of the new aminopyrazole derivatives and their ability to inhibit Aβ_{42}-induced toxicity in cell culture.[21]

RESULTS AND DISCUSSION

Identification of Candidate Interaction Regions. The structure of the Aβ_{42} protofilament, which was experimentally determined by Lührs et al.,[15] gives important information about those candidate regions, which might be targeted by C-terminally extended aminopyrazoles (Figures 1a and 1b). There are at least four regions with distinct structural properties: (a) a polar region, formed by the stretch from D23-K28, (b) the E22 ladder, formed by the E22 side chains of adjacent layers of the cross-β-sheet, (c) the central cleft formed in the interior of the U-shaped turn, and (d) the unpolar region, formed by residues A30-V36 of the C-terminal β-strand.

Anchor Point for Molecular Modeling Studies. In order to design suitable C-terminal extensions, the binding site of the aminopyrazole trimer must first be determined with sufficient accuracy. In the past, detailed conformational NMR analyses between aminopyrazole ligands and the model peptide (K)KLVFF, a putative nucleation site in Aβ, furnished strong hints for direct hydrogen bonds between ligand and peptidic backbone as well as π-stacking interactions with both phenylalanines.[22]

In the present study, near-UV CD measurements of water-soluble trimeric ligands in 1:1 mixtures with Aβ_{42} reveal that in most cases a new CD band evolves at 260−320 nm with a positive maximum at 280 nm, typical for complexes of aromatic moieties (Phe 260−270 nm; Tyr 270−280 nm; Trp 290−300 nm). Since at this wavelength aminopyrazole ligands are CD silent, we attribute the new band to tight complex formation between aromatic units in Aβ and ligand, most likely between the two consecutive phenylalanines (F19/F20) and the pyrazole nuclei. The importance of the $\pi-\pi$-stacking interactions is also confirmed from molecular dynamics simulations, which prove that the respective binding site exhibits a considerably higher conformational stability compared to adjacent binding sites (Supporting Information, Figure S1). These biophysical and computational observations provide the basis for a structural model of the aminopyrazole trimer in complex with the fibrillar form of Aβ_{42}. In this model, the trimer is hydrogen bonded to the solvent-exposed top face of the KLVFF backbone and simultaneously stacks its pyrazole nuclei with both phenylalanines in the form of a hydrophobic cleft (Figure 1).

Design of the C-Terminally Extended Ligand. We attempted to match the main binding regions identified above with complementary recognition sites on the complexing aminopyrazole trimers and to vary sizes and distances from their attachment point. (a) For the polar region (E22−K28) carboxylate and ammonium groups were placed close to the aminopyrazoles. (b) Pentacationic appendices are probes for a potential complexation of the glutamate-22 ladder formed by adjacent layers of parallel β-sheets in the aggregated Aβ (Figures 1a and 1d). (c) The central cleft between the polar and the unpolar region was addressed by a TEG (triethyleneglycol) unit, which also serves as a water-soluble linker for remote recognition events. (d) Unpolar residues (I31−V36) are matched by flexible

dx.doi.org/10.1021/ja107675n |J. Am. Chem. Soc. 2011, 133, 4348–4358

Scheme 1. Lewis Structures of Unprotected Aminopyrazole Trimer Derivatives with Appendices X[a]

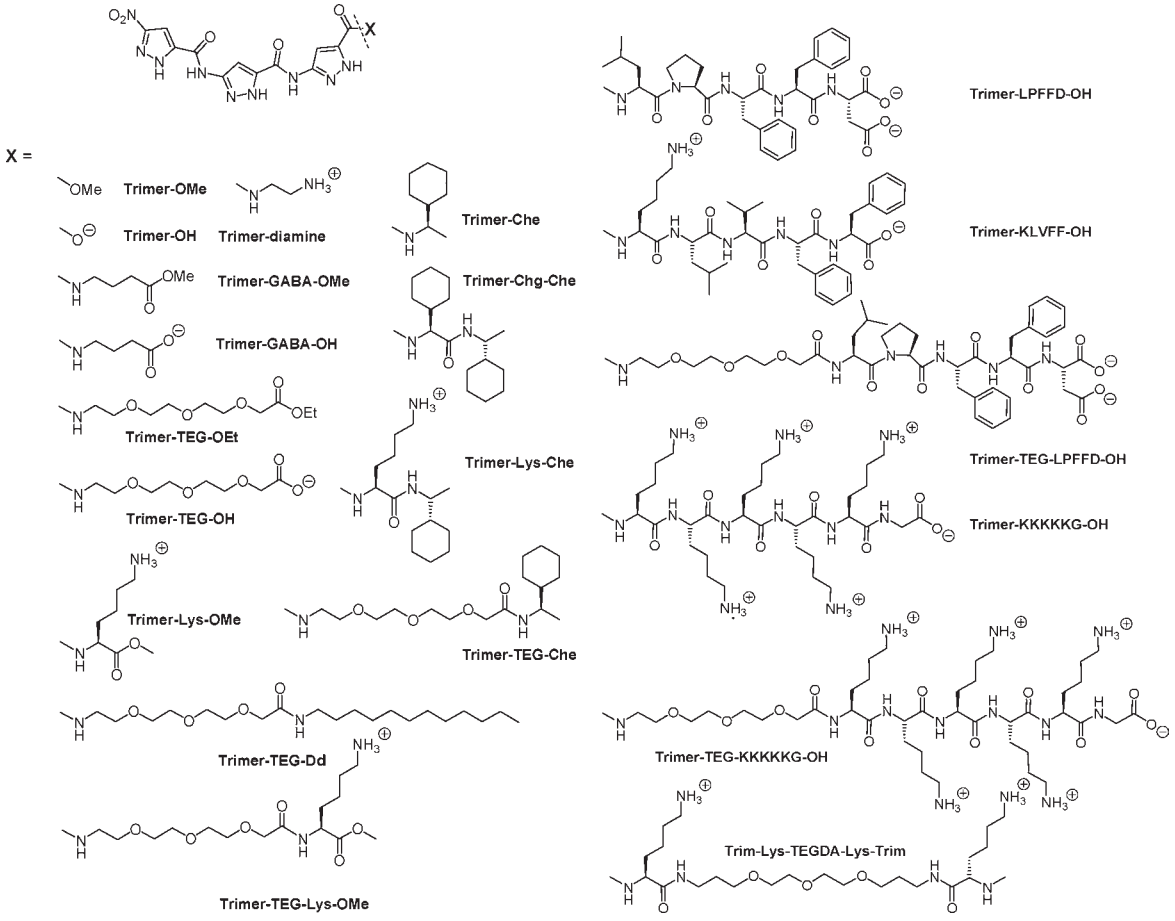

[a] (Left) Small neutral, anionic, and cationic moieties as well as unpolar and TEG-spacer groups. (Right) Peptidic attachments.

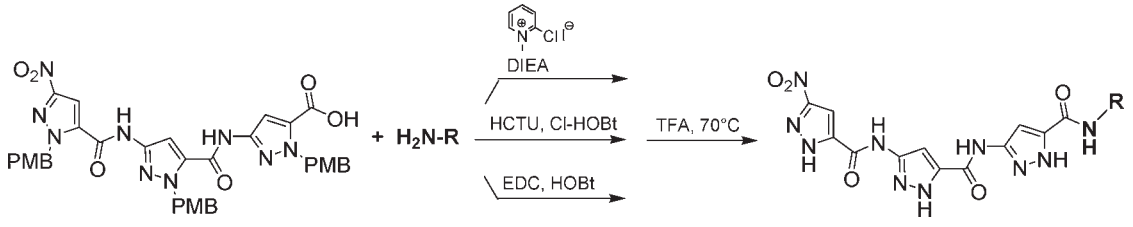

Figure 3. Synthetic access to the new C-terminally modified aminopyrazole trimers via peptide coupling of various amines onto the PMB-protected trimer and final total deprotection.

branched hydrocarbons as found in cyclohexylglycine, already introduced by the Stott group.[8] In addition, small peptide fragments from the central hydrophobic core (CHC) were employed.

In order to investigate whether these extensions are actually capable of interacting with the Aβ_{42} fibril, molecular dynamics simulations were performed for several representative ligands. All computational studies started from the Aβ_{42}-fibril structure obtained from NMR spectroscopic data by Lührs et al.[15] Starting from the aminopyrazole binding site, C-terminally modified ligands were modeled in complex with Aβ_{42} and the mode of interaction was subsequently refined using molecular dynamics simulations (see Supporting Information for details).

Modeling Results. Molecular dynamics simulations of the Aβ_{42} ligand complexes in an explicit solvent environment proved that both the backbone hydrogen bonds as well as the π-stacking interactions of the aminopyrazole moiety remained stable (Supporting Information Figures S1 and S2). Intriguingly, several additional favorable interactions were found for the C-terminally extended trimers, which were typical for each major class of trimer extensions (Figure 2; see Supporting Information Table S2 for a detailed list of the intermolecular interactions formed).

Extended or cyclic unpolar groups align with nonpolar side chains and undergo hydrophobic as well as dispersive interactions (Trimer-Chg-Che, Trimer-K-Che, Trimer-TEG-Dd). According to a conformational search, unpolar binding sites on the ligand indeed prefer the cluster of hydrophobic residues from I31 to V36. A TEG spacer in Trimer-TEG-Dd allows the attached dodecyl tail to explore the entire M35 ladder (formed by adjacent

dx.doi.org/10.1021/ja107675n |J. Am. Chem. Soc. 2011, 133, 4348–4358

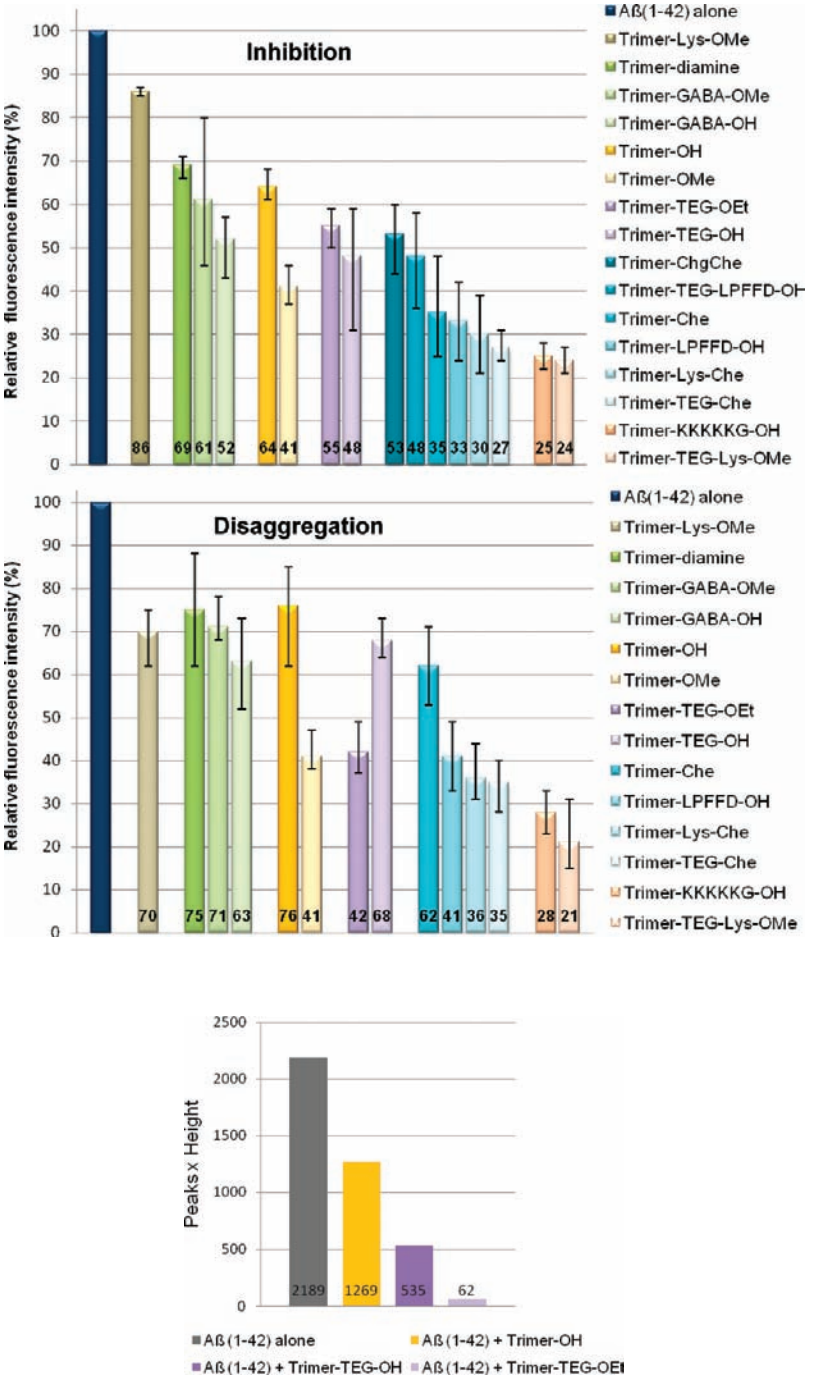

Figure 4. Equilibrium of 33 μM Aβ_{42} aggregation vs disaggregation in the absence or presence of trimeric aminopyrazole inhibitors (each at 198 μM): (top) inhibition of aggregation and (middle) disaggregation (10 mM PBS, pH 7.3). The color code for each aminopyrazole trimer derivative is maintained throughout the entire article. For each bar 6 measurements were averaged. (Bottom) FCS measurements at 5 nm Aβ with Trimer-OH in comparison to Trim-TEG-OH/OEt (each at 100 nM).

layers of parallel β-sheets in the aggregated Aβ) during MD simulations for extended van der Waals interactions on the back of the pentameric Aβ_{42} fibril (Figure 2b). For other nonpolar ligands carrying a cyclohexyl moiety or a TEG-NMe extension, penetration into the central cleft is observed (Figures 2c and 2d). The latter ligands also exhibit the strongest destabilizing effect of the Aβ_{42} fibril (Supporting Information Figure S3).

Aminopyrazole derivatives, which carry one or multiple lysine residues (Trimer-KKKKKG-OH, Trimer-TEG-KKKKKG-OH, Trimer-TEG-K-OH) are capable of interacting with the E22 ladder of Aβ_{42} (Figures 2e and 2f). However, only long tethers allowed simultaneous complexation of more than one carboxylate group of the glutamate ladder by pentalysine attachments. Two polar interactions are observed on average over the entire simulation time for Trimer-TEG-KKKKKG-OH (Supporting Information Tables S2 and S3).

The simulations above suggest that three of the four candidate interaction regions defined in Figure 1a can indeed be targeted by

dx.doi.org/10.1021/ja107675n |*J. Am. Chem. Soc.* 2011, 133, 4348–4358

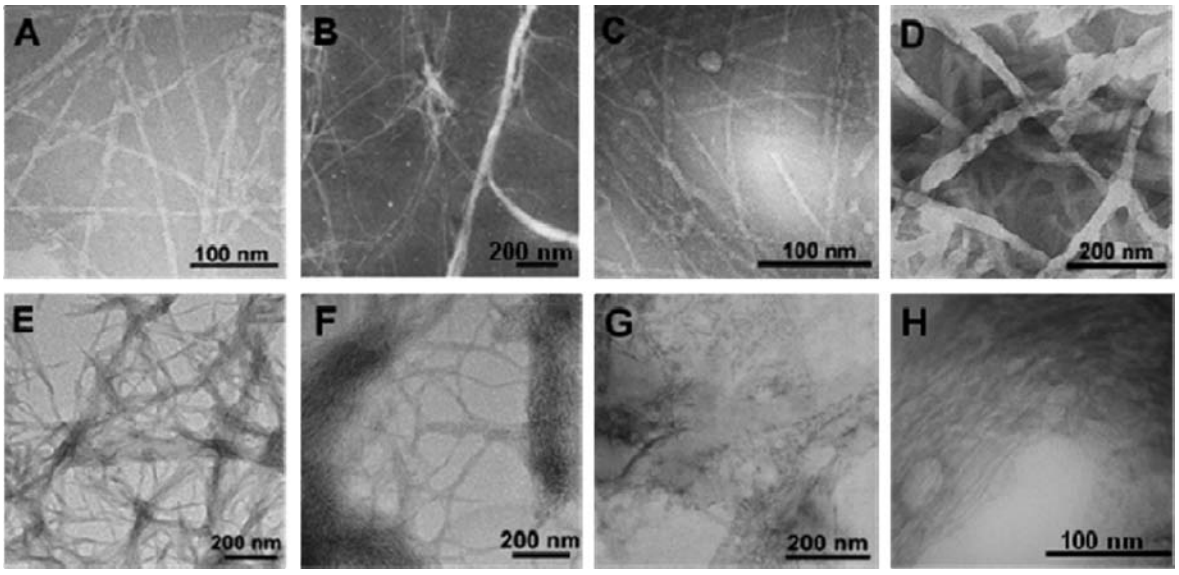

Figure 5. TEM pictures: (A) Aβ(1−42) fibrils; (B−H) Aβ(1−42) mixtures (20 μM) with aminopyrazole trimer derivatives (200 μM) ((B) Trimer-OMe, (C) Trimer-OH, (D) Trimer-Che, (E) Trimer-K-OMe, (F) Trimer-TEG-K-OMe, (G) Trimer-TEG-OEt, (H) Trimer-TEG-OH.)

the C-terminal extensions. Only for the polar region (D23−K28) we observed very few interactions with the ligands. This might be explained by the fact that D23 and K28 form a stable salt bridge, and putative hydrogen bonds with S26/N27 have only a small energetic contribution in the aqueous environment.

Another interesting finding is the fact that the TEG spacer itself forms numerous interactions with the Aβ_{42} fibril in all simulations of TEG-containing derivatives (Supporting Information Table S2). These interactions are formed either with the stretch F20−V24 of the N-terminal β-strand or with I32−L34 of the C-terminal β-strand, suggesting that the TEG spacer itself might play a beneficial role for the anti-Aβ activity of the ligands.

In summary, the MD simulations indicate that different types of extension of the trimer core are capable of targeting different sites on the Aβ_{42} fibril and undergo distinct interactions. To investigate whether these different modes of binding also result in different effects on Aβ aggregation, a large number of new Trimer derivatives was synthesized and experimentally characterized. Scheme 1 shows an overview of all synthesized aminopyrazole derivatives and their chemical classification.

Synthesis. The trimeric aminopyrazole's core structure was elongated with the above-discussed additional binding sites. To this end, its C-terminal carboxylic acid was connected to the respective amines by way of an amide bond. Conventional coupling reagents comprised EDC/HOBt, HCTU/Cl-HOBt, and Mukaiyama's reagent, which produced the hybrid compounds in high yields. In an economic fashion, all protecting groups of the tether were finally cleaved by TFA together with all PMB moieties on the aminopyrazole nuclei. Peptidic tethers were first synthesized by manual solid-phase peptide synthesis (SPPS) on a Wang resin, followed by covalent attachment at the aminopyrazole trimer (HBTU, DIEA). Final deblocking of all acid-labile protecting groups at 70 °C for ∼3 h furnished, after precipitation and recrystallization from ether, analytically pure final products (Figure 3). All these new trimeric aminopyrazoles are soluble in DMSO, most of them also in water.

Aggregation Studies with ThT. The influence of the new β-sheet ligands on the Aβ self-assembly process was first studied thermodynamically using the thioflavine T (ThT) fluorescence assay.[23] Care was taken to eliminate fluorescence changes induced by any other events than the aggregation process; thus, each ligand was separately shown to be nonfluorescent and not to alter ThT fluorescence in mixtures. Controls with pure Aβ (1−42) were identical in peptide concentration as well as buffer and solvent composition.

Table 1. Classification of CD Spectra to Three Main Types

type A (polar)	type B (very polar)	type C (unpolar)
Trim-K-OMe	Trim-KKKKKG-OH	Trim-K-Che
Trim-TEG-K-OMe	Trim-TEG-KKKKKG-OH	Trim-TEG-KLVFF-OH
Trim-TEG-OH	Trim-K-TEGDA-K-Trim	Trim-TEG-Dd

Inhibition. After 72 h, the aggregation process has reached a maximum in the absence or presence of any trimeric ligand. The respective equilibrium concentration then was indicated by the relative fluorescene intensity reached at the predefined end point after 3 days. The full series of new aminopyrazole trimer derivatives was subjected to ThT inhibition experiments, and the final equilibrium was analyzed by comparison of the respective fluorescence intensities of intercalated dye at 482 nm (exc. at 442 nm). Figure 4 (top) reveals a significant structure−activity relation for the ligands with respect to aggregation prevention of Aβ(1−42): structurally related compounds in general display comparable inhibition properties. Two classes of the modified derivatives significantly surpass the original trimer activity: Trimer-Che/Trimer-K-Che/Trimer-LPFFD-OH with attached extended lipophilic groups and Trimer-TEG-K-OMe/Trimer-KKKKKG-OH with a distant or multiple lysine residues. Their proposed mechanism of action is discussed within the next sections together with all the other biophysical and biochemical data.

The strong influence of the spacer unit becomes particularly evident for compounds with a single lysine residue. A single C-terminal lysine directly attached to the trimer (Trim-K-OMe) exhibits very special properties: Contrary to almost all other trimer derivatives, this aminopyrazole accelerates Aβ aggregation (data not shown). On the other hand, Trim-TEG-K-OMe, with a

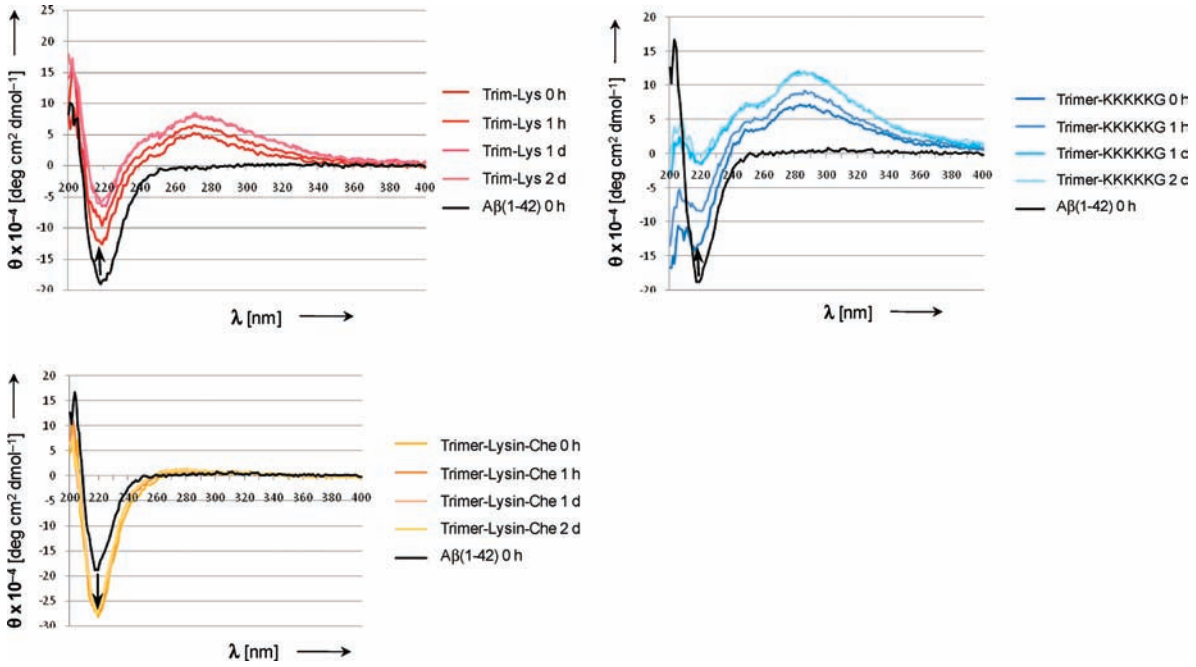

Figure 6. Typical CD spectra recorded for aggregated Aβ(1−42) alone (black) and after addition of aminopyrazole ligand (type A, Trimer-K-OMe: red; type B, Trimer-KKKKKG-OH blue; type C, Trimer-K-Che: brown). Time progresses in the direction of the embedded arrows, indicated by lighter colors (0 h, 1 h, 1d, 2d). Test solutions contained 10 μM Aβ(1−42), 5 μM potassium phosphate buffer (pH = 7.3), 2% HFIP, and 10 μM of the respective aminopyrazole trimer derivative.

Table 2. Cell Viability and IC_{50} Values of the Most Potent inhibitors of Aβ-Induced Toxicity[a]

inhibitor	viability [%]	IC_{50} [μM]
Trim-LPFFD-OH	97	**3.1**
Trim-TEG-LPFFD-OH	113	10.1
Trim-GABA-OH	103	18.5
Trim-GABA-OMe	97	20.3
Trim-K-TEGDA-K-Trim	116	21.5
Trim-TEG-OH	111	35.3
Trim-TEG-K-OMe	117	52.7
Trim-Chg-Che	97	81.0
Trim-TEG-KLVFF-OH	100	>100
Trim-TEG-Dd	108	>100

[a] Aβ lesion control (10 μM) was set at ~75% viability.

single lysine separated from the trimeric aminopyrazole core unit by the TEG spacer, leads to the most efficient suppression of Aβ fibril formation of all tested derivatives (20% ThT fluorescence). This structurally closely related pair of aminopyrazole trimers is a striking example of how strongly the exact placement of binding moieties influences the degree and path of Aβ aggregation.

Disaggregation. Starting from preformed fibrils, the disassembly process was also monitored with the full series of modified trimeric aminopyrazoles (Figure 4). Remarkably, the inhibition pattern (top) looks quite similar to the disaggregation pattern (bottom); in several cases, the total percentage of remaining ThT fluorescence is identical. In other words, little difference is observed between the end points of aggregation assays, in which the ligand inhibits de novo aggregation starting from monomeric Aβ molecules, and those experiments which require disaggregation of preformed fibrils by externally added ligand. Experimental evidence is thus provided for the fact that aminopyrazole ligands operate in a fully reversible fashion and reach an open equilibrium when the thermodynamically most favorable complex is formed. The total reduction in Aβ aggregate concentration by the trimer parent compound corresponds to an estimated dissociation constant of the respective complex in the low micromolar range (2 μM K_d in PBS buffer).

Colloidal Mechanism? It might be argued that the observed effect could in principle also stem from colloidal aggregates, which have been shown to inhibit amyloid polymerization in prion proteins in an unspecific way.[24] To clarify this point, extensive DLS measurements were carried out in combination with AFM and DOSY experiments as well as cmc determinations (all experiments in the Supporting Information). With one exception (Trimer-TEG-K-OMe) none of our new ligands forms colloids, which is further corroborated by inspection of TEM images of the pure compounds. Even this ligand did not show a colloidal mechanism, when we transferred the established tests for colloidal inhibition from prion protein to seeded Aβ aggregation.

The structural influence of differently modified trimer derivatives on Aβ aggregation was now further studied with fluorescence correlation spectroscopy (FCS), sedimentation velocity analysis (SVA, based on analytical ultracentrifugation), and transmission electron microscopy (TEM).

Fluorescence Correlation Spectroscopy. In the FCS experiment a 5 nM Oregon-Green-labeled $A\beta_{42}$ solution was prepared in PBS buffer with ~3% DMSO.[25] These Aβ concentrations are also found in the human brain.[26−28] Trimer-OH was added at 100 nM and reduced the peaks × height value to ~60% of the control. Since the number of peaks remained unchanged, their molecular weight was significantly reduced.[29] Much more pronounced is the influence of Trimer-TEG derivatives: FCS here witnesses the uniform transition to very small oligomers within all Aβ aggregates (Figure 4, bottom). This observation

dx.doi.org/10.1021/ja107675n |J. Am. Chem. Soc. 2011, 133, 4348–4358

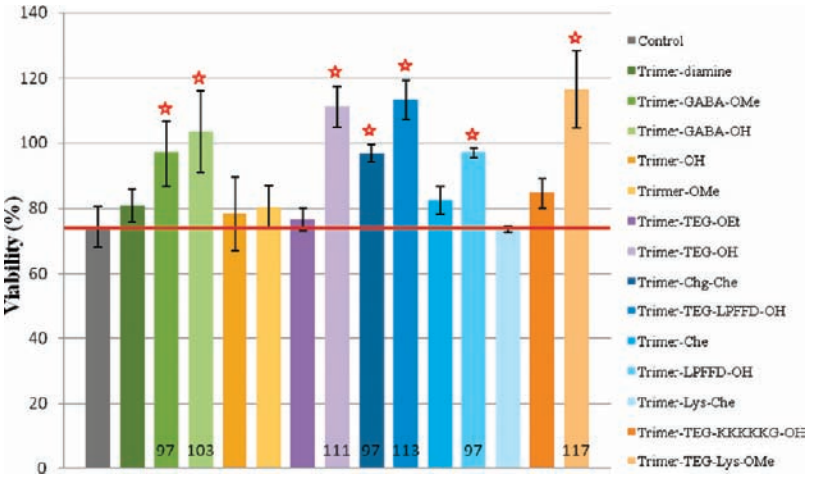

Figure 7. Viability assays of PC-12 cells with trimeric aminopyrazoles (100 μM). Aβ lesion control (10 μM) was set at ~75% viability. Most effective drugs are marked with asterisks.

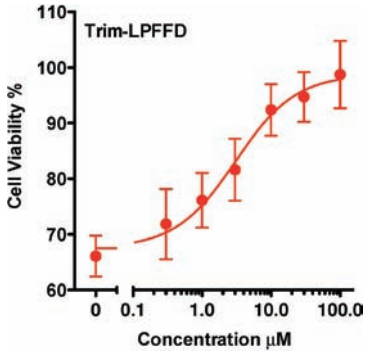

Figure 8. Dose−response curve for inhibition of Aβ-induced toxicity in PC-12 cells by Trimer-LPFFD (IC_{50} = 3.1 μM).

underlines the overall beneficial effect of the TEG spacer on the antiaggregation potency of the ligands. In addition, the differences between Trimer-TEG-OH and Trimer-TEG-OEt indicate that the polarity of the extension also plays an important role for the interaction with the $A\beta_{42}$ fibril. This is in line with the numerous interactions observed for Trimer-TEG-NMe in the modeling study (Figure 2d and Supporting Information Table S2).

Sedimentation Velocity Analysis. Markedly different behavior was also observed for various classes of modified aminopyrazole trimers in ultracentrifugation experiments with Oregon-Green-labeled Aβ:[30] weight-averaged sedimentation coefficients for pure Aβ were about 50 S, whereas those for its complex with Trimer-OH continuously decreased in a dose-dependent manner down to 25S, corresponding to a 50% molecular weight reduction (Supporting Information Figures S4 and S5).[31] By contrast, the TEG-elongated aminopyrazole trimer does not significantly change the medium aggregate size of aggregated Aβ but instead produces a significant amount of smaller oligomers (monomers−18mers). On the other extreme, the exceptionally high aggregation propensity of Trim-K-OMe is also well documented in sedimentations, featuring the total loss of soluble Aβ-peptide signal during rotor acceleration. For all these trimer derivatives, sedimentation assays prove direct complex formation with Aβ.[32]

Transmission Electron Microscopy. A broad spectrum of different morphologies were produced in complexes between various kinds of aminopyrazole trimers and Aβ (Figure 5). TEM pictures were obtained from mature Aβ fibrils (>600 nm long) as well as globular particles (3−30 nm diameter), grown in the absence of aminopyrazole ligands.[33]

While twisted fibrils from pure Aβ had a diameter of 10 nm, thin filaments were produced in the presence of the Trimer-OH (5 nm diameter) and the number of mature fibrils was greatly reduced. We tentatively conclude that the trimer seems to break the mature fibrils into protofilaments by a combination of backbone recognition and hydrophobic interactions. The unpolar Trimer-Che, on the other hand, produced very thick twisted fibrils (up to 70 nm), with a length of at least 600 nm. It thus seems that here fibrillogenesis is not prevented but rather shifted to a much more compact form, which does not accommodate well-ordered fluorescent ThT molecules. TEM pictures of mixtures of aggregation accelerator Trimer-K-OMe with Aβ show very thin fibrils (5−10 nm) of 800 nm length, while Trimer-TEG-K-OMe redirects the aggregation process of Aβ to unstructured material and thin bent filaments, distinct from Aβ fibrils. Finally, from Aβ solutions in the presence of Trim-TEG-OH or -OMe, very thin, delicate structures evolve, which show no helical twist. In total, similar appendices again produced similar TEM morphologies of aggregated material, which must originate from their similar complexation behavior.

CD Spectroscopy. CD spectra could only be measured from Aβ complexes with the most soluble aminopyrazole trimers. None of the examined ligands had its own CD spectrum above 210 nm, so that spectral changes could be directly attributed to interactions between Aβ and the respective ligand. They can be divided into 3 groups (Table 1, Figure 6): Type A is found for derivatives with a single lysine or TEG spacer only; it is characterized by an induced CD in the aromatic region around 280 nm, without a significant loss of β-sheet conformation. Type B is obtained with the most polar derivatives which contain multiple lysine residues; these are the most potent of all synthesized aminopyrazole derivatives and deplete the ThT fluorescence level down to 20% in inhibition and disaggregation experiments (Figure 4). The corresponding CD spectrum features again the additional CD band at ~280 nm, typical for aromatic amino acids; however, in this case, the β-sheet band almost completely disappears with time, indicating dissolution of the secondary peptide structure.

dx.doi.org/10.1021/ja107675n |*J. Am. Chem. Soc.* 2011, 133, 4348–4358

Table 3. Synopsis of All Experimental Results Ordered by Ligand Classes

experiment	E22 ladder (polylysines)	polar region (single charged groups)	unpolar region (extended alkyl residues)	central pore (TEG derivatives)
ThT (inhibition)[a]	24%	25%	27−50%	48−54%
ThT (disaggregation)[a]	28%	21%	35−62%	42−68%
FCS[b]				3−21%
sedimentation[c]	50S+	50S+	50S+	5−10S + 50S
TEM[d]	amorphous material	unstructured material + thin bent filaments	thick twisted fibrils (70 nm × 600 nm)	very thin, delicate structures
CD[e]	ICD (280 nm); no β-sheet (218 nm)	ICD (280 nm), less β-sheet (218 nm)	increased β-sheet band	ICD (280 nm), less β-sheet (218 nm)
MTT[f]	IC_{50} > 80 μM	$IC_{50} \geq$ 22 μM	$IC_{50} \geq$ 3 μM	$IC_{50} \geq$ 35 μM

[a] Percent ThT fluorescence of a 6:1 mixture relative to $A\beta_{42}$ control (10 μM). [b] Percent OregonGreen fluorescence of a 20:1 mixture relative to $A\beta_{42}$ control (5 nM). [c] 10:1 mixture; $A\beta_{42}$ control (20 μM) shows only 50S particles. [d] Ten-fold diluted sedimentation samples. [e] 1:1 mixture with $A\beta_{42}$ (10 μM each). [f] PC-12 cells with $A\beta_{42}$ lesion (10 μM).

CD spectra of Trimer-K-Che, Trimer-TEG-KLVFF-OH, and Trimer-TEG-DD all feature/display an almost doubled β-sheet band intensity and the total loss of the aromatic signal at 280 nm (type C). A straightforward interpretation suggests a remarkable stabilization of the cross-β-sheet (in line with TEM results) with concomitant withdrawal of the aminopyrazole from its Phe-Phe cleft.

Although it is tempting to correlate CD spectra with modeling structures, it should be kept in mind that the time regimes are drastically different: while MD simulations last only for a few nanoseconds and would rather represent structures formed in the early stages of fibril disassembly, the CD spectra as well as ThT assays cover several days, including potential major conformational rearrangements.

Inhibition of Aβ-Induced Toxicity. Initially, all compounds were screened for any toxic effect they might have by adding each compound at 100 μM and measuring the effect on cell viability using the 3-(4,5-dimethylthiazol-2-yl)-2,5-diphenyltetrazolium bromide (MTT) reduction assay[34] in differentiated rat pheochromocytoma (PC-12) cells.[35] Encouragingly, none of the compounds was toxic to the cells at this concentration. Next, to examine whether the aminopyrazole trimers could protect from Aβ42-induced neurotoxicity, cells were treated for 24 h with 10 μM Aβ(1−42) in the absence or presence of 100 μM of each compound. The viability of untreated cells decreased by 30−40% (MTT). Inhibition of Aβ(1−42)-induced toxicity by Trimer-OH/OMe was very moderate (<10% viability increase); however, many of the new derivatives achieved a complete rescue of cell viability (Table 2, Figure 7).

Intriguingly, the most efficient inhibition of Aβ toxicity was achieved with 3 lipophilic extensions and Trimer-TEG-K-OMe, which were also superior in ThT and related assays. The two GABA derivatives are a surprise; they might potentially interact with GABA receptors and not with the Aβ peptide itself. The above-delineated findings demonstrate that trimeric aminopyrazoles are indeed active against Aβ-induced toxicity in living cells; they also provide experimental evidence for their low toxicity at relatively high doses of 0.1 mM, inspite of, e.g., the presence of an N-terminal nitro group.

On the basis of this initial screen, we decided to evaluate the IC_{50} value of compounds that increased the viability of PC-12 cells to ≥90%. The data are summarized in Table 2. To determine the IC_{50} value of each of the compounds, dose-dependence MTT experiments were conducted with the aminopyrazole trimers at a fixed $A\beta_{42}$ concentration of 10 μM and increasing concentrations of β-sheet ligand (0.3, 1, 3, 10, 30, and 100 μM). IC_{50} in this respect is defined as the concentration of the β-sheet ligand (aminopyrazole trimer derivative), at which the inhibition of Aβ toxicity just reaches 50% (Figure 8).

With respect to IC_{50} values, the two nonpolar LPFFD derivatives were now found to be the most effective. Since the $A\beta_{42}$ concentration was always kept constant at 10 μM, it should be emphasized that substoichiometric IC_{50} values such as that of Trim-LPFFD-OH indicate very high affinity toward the target peptide, even if a 1:1 complex is assumed. A 3 μM IC_{50} value is a remarkable number by itself and testifies to an efficient disaggregation capability in the cell environment. It should be kept in mind that in the brain Aβ concentrations are in the low nanomolar range, similar to the situation in enzyme assays. Only in such a scenario, IC_{50} values can be expected to drop to nanomolar concentrations.

CONCLUSIONS AND OUTLOOK

This investigation provides experimental evidence for the fact that small structural changes in β-sheet ligands can have a profound influence on the aggregation behavior of misfolding proteins. Only one of all examined aminopyrazole ligands forms colloids, and none displayed the characteristics of a colloidal mechanism, so that direct interaction of amyloid peptide with monomeric ligand species can be assumed. Moreover, a common anchor point (F19−F20) could be identified, allowing one to perform docking experiments and subsequent MD simulations. Intriguingly, various types of computationally designed binding sites on the ligands allow tight interactions with specific Aβ regions (cf. MD simulations) and correlate well with different kinds of modulated Aβ aggregation behavior, throughout the entire series of analytical experiments, Table 3.

It should however be emphasized that MD simulations treat only a very short time span in the beginning of the aminopyrazoles' interactions with Aβ. CD measurements as well as ThT aggregation assays on the other hand display pronounced continuous changes within more than 2 h, which may involve conformational changes that are not yet visible even during extended molecular dynamics simulations. A preliminary structure−activity relation can therefore be suggested only with great care, evolving from the combination of different biophysical, biochemical, and "in silico" experiments. Two major binding motifs were discovered, which greatly improve the β-sheet

breaker ability of the aminopyrazole trimer: remote lipophilic moieties for dispersive interactions with the nonpolar cluster of amino acids between I31 and V36[36] and distant polyLys stretches which interact with the E22 ladder. Only the latter, however, effectively destroys the cross-β-sheet (CD, TEM). In addition, the TEG spacer was found to play an active role in destabilizing the turn of the U-shaped protofilament (Trim-TEG-OMe; Trim-TEG-K-OMe). Importantly, only the synopsis of ThT assay, sedimentation experiment, and TEM picture allows one to draw conclusions about the aggregate species formed by direct interaction between Aβ and the aminopyrazole trimer derivatives: In most cases the content of well-ordered soluble fibrils is greatly diminished (ThT), because these are transformed into less structured aggregates with a high molecular weight (UC). The few remaining fibrillar components display a significantly altered morphology (TEM) and have lost their acute cellular toxicity (MTT). We will in the future try to confirm these structure motifs postulated from modeling and aggregation experiments. Direct evidence should be gained from cocrystals of these complexes as well as from 2D solid-state NMR experiments.

■ ASSOCIATED CONTENT

Supporting Information. Detailed synthetic experimental procedures, computational studies, thioflavine T-assays, determination of the equilibrium from inhibition and disaggregation experiments, colloid experiments, UV−vis extinctions, DLS, AFM, DOSY, cmc determination, seeded aggregations, CD-spectroscopic measurements, FCS, sedimentation analysis, transmission electron microscopy, and MTT viability assays. This material is available free of charge via the Internet at http://pubs.acs.org.

■ AUTHOR INFORMATION

Corresponding Author
Thomas.Schrader@uni-due.de.

■ ACKNOWLEDGMENT

Financial support from the American Health Assistance Foundation (grant A2008-350) and the UCLA Jim Easton Consortium for Alzheimer's Drug Discovery and Biomarker Development is gratefully acknowledged. This work was also supported by the Deutsche Forschungsgemeinschaft and the Volkswagen foundation.

■ REFERENCES

(1) Review: Jakob-Roetne, R.; Jacobsen, H. *Angew. Chem., Int. Ed.* **2009**, *48*, 3030–3059.

(2) Bisstyrylbenzenes: Flaherty, D. P.; Walsh, S. M.; Kiyota, T.; Dong, Y.; Ikezu, T.; Vennerstrom, J. L. *J. Med. Chem.* **2007**, *50*, 4986–4992. (b) Porat, Y; Abramowitz, A.; Gazit, E. Y. *Chem. Biol. Drug Des.* **2006**, *67*, 27–37.

(3) Yang, F.; Lim, G. P.; Begum, A. N.; Ubeda, O. J.; Simmons, M. R.; Ambegaokar, S. S.; Chen, P. P.; Kayed, R.; Glabe, C. G.; Frautschy, S. A.; Cole, G. M. *J. Biol. Chem.* **2005**, *280*, 5892–5901.

(4) Zn and Cu chelators:Cherny, R. A.; Atwood, C. S.; Xilinas, M. E.; Gray, D. N.; Jones, W. D.; McLean, C. A.; Barnham, K. J.; Volitakis, I.; Fraser, F. W.; Kim, Y. *Neuron* **2001**, *30*, 665–676.

(5) KLVFF derivatives: (a) Tjernberg, L. O.; Naslund, J.; Lindqvist, L.; Johansson, J.; Karlstrom, A. R.; Thyberg, J.; Terenius, L.; Nordstedt, C. *J. Biol. Chem.* **1996**, *271*, 8545–8548. (b) Austen, B. M.; Paleologou, K. E.; Ali, S. A. E.; Qureshi, M. M.; Allsop, D.; El-Agnaf, O. M. A. *Biochemistry* **2008**, *47*, 1984–1992. (c) KLVFF aggregation and gelation: Krysmann, M. J.; Castelletto, V.; Kelarakis, A.; Hamley, I. W.; Hule, R. A.; Pochan, D. J. *Biochemistry* **2008**, *47*, 4597–4605.

(6) Soto, C.; Sigurdsson, E. M.; Morelli, L.; Kumar, R. A.; Castaño, E. M.; Frangione, B. *Nat. Med.* **1998**, *4*, 822–826.

(7) Gordon, D. J.; Meredith, S. C. *Biochemistry* **2003**, *42*, 475–485. Hughes, E.; Burke, R. M.; Doig, A. J. *J. Biol. Chem.* **2000**, *275*, 25109–25115. Kapurniotu, A.; Schmauder, A.; Tenidis, K. *J. Mol. Biol.* **2002**, *315*, 339–350.

(8) Kokkoni, N.; Stott, K.; Amijee, H.; Mason, J. M.; Doig, A. J. *Biochemistry* **2006**, *45*, 9906–9918.

(9) Aisen, P. S; Saumier, D.; Briand, R.; Laurin, J.; Gervais, F.; Tremblay, P.; Garceau, D. A. *Neurology* **2006**, *67*, 1757–63. Wright, T. M. *Drugs Today* **2006**, *42*, 291–298 (Homotaurin dropped out of phase III clinical trial).

(10) (a) McLaurin, J.; Goloumb, R.; Jurewicz, A.; Antel, J. P.; Fraser, P. E. *J. Biol. Chem.* **2000**, *275*, 18495–18502. (b) McLaurin, J.; Kierstead, M. E.; Brown, M. E.; Hawkes, C. A.; Lambermon, M. H. L.; Phinney, A. L.; Darabie, A. A.; Cousins, J. E.; French, J. E.; Lan, M. F.; Chen, F.; Wong, S. S. N.; Mount, H. T. J.; Fraser, P. E.; Westaway, D.; St. George-Hyslop, P. *Nat. Med.* **2006**, *12*, 801–808.

(11) Ehrnhoefer, D. E.; Bieschke, J.; Boeddrich, A.; Herbst, M.; Masino, L.; Lurz, R.; Engemann, S.; Pastore, A.; Wanker, E. E. *Nat. Struct. Mol. Biol.* **2008**, *15*, 558–566.

(12) Structure of an affibody/Aβ40 complex: Hoyer, W.; Gronwall, C.; Jonsson, A.; Stahl, S.; Hard, T. *Proc. Natl. Acad. Sci. U.S.A.* **2008**, *105*, 5099–5104. Hoyer, W.; Hard, T. *J. Mol. Biol.* **2008**, *378*, 398–411.

(13) Sato, T.; Kienlen-Campard, P.; Ahmed, M.; Liu, W.; Li, H. L.; Elliott, J. I.; Aimoto, S.; Constantinescu, S. N.; Octave, J. N.; Smith, S. O. *Biochemistry* **2006**, *45*, 5503–5516.

(14) Petkova, A. T.; Ishii, Y.; Balbach, J. J.; Antzutkin, O. N.; Leapman, R. D.; Delaglio, F.; Tycko, R. *Proc. Natl. Acad. Sci. U.S.A.* **2002**, *99*, 16742–16747. Petkova, A. T.; Yau, W. M.; Tycko, R. *Biochemistry* **2006**, *45*, 498–512.

(15) Lührs, T.; Ritter, C.; Adrian, M.; Riek-Loher, D.; Bohrmann, B.; Dobeli, H; Schubert, D.; Riek, R. *Proc. Natl. Acad. Sci. U.S.A.* **2005**, *102*, 17342–17347.

(16) Ma, B.; Nussinov, R. *Curr. Opin. Chem. Biol.* **2006**, *10*, 445–452. Sato, T.; Kienlen-Campard, P.; Ahmed, M.; Liu, W.; Li, H.; Elliott, J. I.; Aimoto, S.; Constantinescu, S. N.; Octave, J. N.; Smith, S. O. *Biochemistry* **2006**, *45*, 5503–5516.

(17) Schrader, T.; Kirsten, C. *J. Chem. Soc., Chem. Commun.* **1996**, 2089. Schrader, T.; Kirsten, C. N. *J. Am. Chem. Soc.* **1997**, *119*, 12061–12068.

(18) (a) Rzepecki, P.; Wehner, M.; Molt, O.; Zadmard, R.; Schrader, T. *Synthesis* **2003**, 1815–1826. (b) Černovská, K.; Kemter, M.; Gallmeier, H.-C.; Rzepecki, P.; Schrader, T.; König, B. *Org. Biomol. Chem.* **2004**, *2*, 1603–1611. (c) Rzepecki, P.; Gallmeier, H.; Geib, N.; Cernovska, K.; König, B.; Schrader, T. *J. Org. Chem.* **2004**, *69*, 5168–5178. (d) Rzepecki, P.; Geib, N.; Peifer, M.; Biesemeier, F.; Schrader, T. *J. Org. Chem.* **2007**, *72*, 3614–3624.

(19) (a) Rzepecki, P.; Nagel-Steger, L.; Feuerstein, S.; Linne, U.; Molt, O.; Zadmard, R.; Aschermann, K.; Wehner, M.; Schrader, T.; Riesner, D. *J. Biol. Chem.* **2004**, *279*, 47479–47505. (b) Fricke, H.; Funk, A.; Schrader, T.; Gerhards, M. *J. Am. Chem. Soc.* **2008**, *130*, 4692–4698. (c) Fricke, H.; Gerlach, A.; Unterberg, C.; Wehner, M.; Schrader, T.; Gerhards, M. *Angew. Chem.* **2009**, *48*, 900–904.

(20) Biesemeier, F.; K. Hochdörffer, L. Nagel-Steger, Riesner, D.; Schrader, T.; . DE 10 2006 015 140.2, Patent application March 28, 2006.

(21) This study was conducted with Aβ_{42}, which is far more aggressive than Aβ_{40}; however, since both peptides contain the same well-oriented central peptide fragment, we expect the inhibitors to work just as well for Aβ_{40}.

(22) Rzepecki, P.; Schrader, T. *J. Am. Chem. Soc.* **2005**, *127*, 3016–3025.

(23) LeVine, H., III *Methods Enzymol.* **1999**, *309*, 274–284.

(24) Feng, B. Y.; Toyama, B. H.; Wille, H; Colby, D. W; Collins, S. R.; May, B. C. H.; Prusiner, S. B.; Weissman, J.; Shoichet, B. K. *Nat. Chem. Biol.* **2008**, *4*, 197–199.

(25) Chang, L.; Bakhos, L.; Wang, Z.; Venton, D. L.; Klein, W. L. *J. Mol. Neurosci.* **2003**, *20*, 305–313.
(26) Haass, C.; Schlossmacher, M. G.; Hung, A. Y.; Vigo-Pelfrey, C.; Mellon, A.; Ostaszewski, B. L. *Nature* **1992**, *359*, 322–325.
(27) Shoji, M.; Golde, T. E.; Ghiso, J.; Cheung, T. T.; Estus, S.; Shaffer, L. M. *Science* **1992**, *258*, 126–129.
(28) Seubert, P.; Vigo-Pelfrey, C.; Esch, F.; Lee, M.; Dovey, H.; Davis, D. *Nature* **1992**, *359*, 325–327.
(29) The Aβ concentration is well below Aβ's cmc:Klajnert, B.; Cortijo-Arellano, M.; Bryszewska, M; Cladera, J. *Biochem. Biophys. Res. Commun.* **2006**, *339*, 577–582.
(30) *Molecular Probes*; Invitrogen: Karlsruhe, Germany.
(31) Demeler, B.; van Holde, K. E. *Anal. Biochem.* **2004**, *335*, 279–288.
(32) Demeler, B.; Brookes, E.; Nagel-Steger, L. *Methods Enzymol.* **2009**, *454*, 87–113.
(33) Nagel-Steger, L.; Demeler, B.; Meyer-Zaika, W.; Hochdörffer, K.; Schrader, T.; Willbold, D. *Eur. Biophys. J.* **2009**, *Feb*, 24.
(34) Datki, Z.; Juhasz, A.; Galfi, M.; Soos, K.; Papp, R.; Zadori, D.; Penke, B. *Brain Res. Bull.* **2003**, *62*, 223–229.
(35) Shearman, M. S. *Methods Enzymol.* **1999**, *309*, 716–723.
(36) The most powerful inhibitor of Aβ-induced toxicity Trimer-TEG-LPFFD-OH uses the well-known β-sheet-breaker motif introduced by Soto et al.